

## Validating Phase-Space Methods with Tensor Networks in Two-Dimensional Spin Models with Power-Law Interactions

Sean R. Muleady<sup>1,2,\*</sup>, Mingru Yang<sup>3,4,\*</sup>, Steven R. White<sup>3</sup>, and Ana Maria Rey<sup>1,2</sup>

<sup>1</sup>*JILA, National Institute of Standards and Technology and Department of Physics, University of Colorado, Boulder, Colorado 80309, USA*

<sup>2</sup>*Center for Theory of Quantum Matter, University of Colorado, Boulder, Colorado 80309, USA*

<sup>3</sup>*Department of Physics and Astronomy, University of California, Irvine, California 92697, USA*

<sup>4</sup>*University of Vienna, Faculty of Physics, Boltzmannngasse 5, 1090 Wien, Austria*

 (Received 31 May 2023; accepted 7 September 2023; published 13 October 2023)

Using a recently developed extension of the time-dependent variational principle for matrix product states, we evaluate the dynamics of 2D power-law interacting  $XXZ$  models, implementable in a variety of state-of-the-art experimental platforms. We compute the spin squeezing as a measure of correlations in the system, and compare to semiclassical phase-space calculations utilizing the discrete truncated Wigner approximation (DTWA). We find the latter efficiently and accurately captures the scaling of entanglement with system size in these systems, despite the comparatively resource-intensive tensor network representation of the dynamics. We also compare the steady-state behavior of DTWA to thermal ensemble calculations with tensor networks. Our results open a way to benchmark dynamical calculations for two-dimensional quantum systems, and allow us to rigorously validate recent predictions for the generation of scalable entangled resources for metrology in these systems.

DOI: [10.1103/PhysRevLett.131.150401](https://doi.org/10.1103/PhysRevLett.131.150401)

The understanding of how quantum correlations develop and propagate during time evolution in interacting many-body systems is a fundamental requirement for next-generation quantum technologies. While considerable work has been devoted to studying such behavior in short-ranged systems, the relatively recent experimental realization of controllable spin systems exhibiting long-ranged interactions, e.g., trapped ions [1–3], polar molecules [4,5], magnetic dipoles [6], and Rydberg atoms [7], has increasingly galvanized efforts to explore and characterize their utility as a quantum resource.

Despite these great opportunities, progress has been slow largely due to the lack of theoretical and numerical tools suited to faithfully characterize long-range interactions, especially in higher dimensions. The exponential growth of the size of Hilbert space with particle number typically excludes exact solutions beyond a few dozen spins. Perturbative techniques are generally restricted to short times [8] or near equilibrium systems, while quasiexact methods based on tensor network techniques have traditionally been limited to short-ranged, one-dimensional systems [9]. A host of approximate methods have been developed for this purpose, with varying ranges of applicability, including clusterization methods [10,11], variational ansatzes [12,13], and efficiently solved phase-space methods [14–18], but the involved approximations are typically uncontrolled, and thus ultimately remain to be validated by other theoretical techniques or experiments.

Here, we demonstrate the utility of both tensor network methods and approximate discrete phase-space methods for studying the far-from-equilibrium collective dynamics of two-dimensional (2D) spin models with a varying range of interactions. We use a recently developed tensor network scheme based on the time-dependent variational principle (TDVP) [19] to solve for the collective spin dynamics of the 2D  $XXZ$  model exhibiting power-law decaying interactions. We demonstrate that the discrete truncated Wigner approximation (DTWA) [15,18] efficiently and accurately captures the collective spin dynamics and buildup of entanglement across a wide range of parameter space, in many cases even yielding improving agreement for larger system sizes. While the large dynamical growth of entanglement eventually limits the system sizes and time accessible by TDVP, DTWA accurately captures the many-body dynamics at comparatively no computational cost, paving the way for its reliable use in theoretical calculations for experimentally relevant system sizes and timescales [20]. Our results directly corroborate a host of recent theoretical predictions relating to the generation of entanglement for metrological applications in power-law interacting spin arrays [12,21–24], which have been experimentally realized in a variety of atomic platforms [25–27].

We further investigate the scrambling and relaxation behavior, computing the entanglement dynamics and expected thermalization temperature for this system. Though DTWA appears to capture the initial relaxation for all the investigated models, it diverges from exact

calculations at long timescales for sufficiently local systems. This observation indicates the breakdown of this method for capturing thermalization in short-range interacting models. Nevertheless, our results validate the utility of DTWA for studying far-from-equilibrium dynamics of long-range, higher-dimensional spin models.

*Model.*—We consider a system of  $N$  spin-1/2 particles, with dynamics governed by the 2D power-law interacting XXZ Hamiltonian

$$\hat{H}_{\text{XXZ}} = -J^\perp \sum_{i < j}^N \frac{\hat{s}_i \cdot \hat{s}_j + \Delta \hat{s}_{z,i} \hat{s}_{z,j}}{|\mathbf{r}_i - \mathbf{r}_j|^\alpha}. \quad (1)$$

$\hat{s}_{\mu,i}$  with  $\mu = x, y, z$  are spin-1/2 operators for the spin at position  $\mathbf{r}_i$ , and we assume a square lattice with open boundary conditions. We also define collective spin operators  $\hat{S}_\mu = \sum_{i=1}^N \hat{s}_{\mu,i}$ , and total spin  $\hat{S}^2 = \sum_{\mu=x,y,z} \hat{S}_\mu^2$ . The Hamiltonian consists of spin-aligning terms  $\hat{s}_i \cdot \hat{s}_j$ , as well as Ising interactions  $\hat{s}_{z,i} \hat{s}_{z,j}$  of relative strength  $\Delta$ . This canonical model of quantum magnetism with power-law couplings plays a key role in describing the relevant physics for many quantum simulation platforms, including trapped ion arrays ( $0 \leq \alpha \leq 3$ ) [3], Rydberg atoms ( $\alpha = 3, 6$ ) [7], magnetic dipoles [6] and polar molecules ( $\alpha = 3$ ) [4], and arrays of neutral atoms ( $\alpha = \infty$ ) [28].

We consider the spin dynamics under Eq. (1) for an initial coherent spin state  $|\psi_0\rangle = |\rightarrow \dots \rightarrow\rangle$ , consisting of all spins polarized along  $+x$ . In the case of all-to-all interactions with  $\alpha = 0$  or in the limit  $\Delta = 0$ , Eq. (1) conserves the total spin, and the state remains in the collective manifold of permutation-symmetric states. For  $\alpha = 0$ , the dynamics of our initial state can be described by the canonical, fully collective one-axis-twisting (OAT) model,  $\hat{H}_{\text{OAT}} = \chi \hat{S}_z^2$  [29]. Additionally, in the Ising limits of  $\Delta \rightarrow \pm\infty$ , the local magnetization is conserved, enabling an analytic solution for the dynamics of arbitrary two-body correlators [30]. However, away from these solvable limits, the dynamics generically involve the larger space of noncollective states.

*Methods.*—An efficient approximation to the dynamics of Eq. (1) is afforded by the DTWA [15,18,31], which provides a way to simulate the dynamics of large, interacting spin systems with a complexity polynomial in  $N$ . This semiclassical phase-space method relies on the classical evolution of independent phase-space trajectories, whose initial conditions are sampled in such a way as to exactly reproduce, within sampling error, the quantum noise distribution of an initial product state, as shown in the Supplemental Material [32]. This method, and closely related variations, have been increasingly utilized in recent years for studies ranging from the universal properties of quantum systems [38,39] to predictions for entanglement-based sensing protocols [21–24]. Ultimately however, the involved approximations remain strictly valid only at short

times, and the resulting predictions remain to be verified by alternative methods or experiments [31,40].

As a more controlled yet intensive approach to solving the quantum dynamics, one can employ the TDVP [41–43], which time evolves a matrix product state (MPS) [9] by variationally minimizing the distance  $\|\hat{H}|\psi\rangle - i(d/dt)|\psi\rangle\|$  at each time within the tangent space of the MPS  $|\psi\rangle$ . Compared with other MPS time-evolution methods in the presence of long-range interactions, TDVP can retain a smaller time step error [19] but may accumulate large errors from projecting into the tangent space of a compressed MPS, whose number of variational parameters may be insufficient to accurately describe the evolution. To resolve this issue, we utilize a global subspace expansion (GSE) method [19], which extends the bond basis of the MPS at the current time with MPS representations of state vectors in the order- $k$  Krylov subspace,

$$\mathcal{K}_k(\hat{H}, |\psi\rangle) = \text{span}\{|\psi\rangle, \hat{H}|\psi\rangle, \dots, \hat{H}^k|\psi\rangle\}. \quad (2)$$

This basis expansion enables us to more efficiently and accurately capture the relevant, developing correlations between spatially distant spins in Eq. (1). Nonetheless, as with any MPS method, it remains challenging to reliably evolve to long times owing to the fast bond dimension growth resulting from entanglement generation, particularly in higher spatial dimensions, as shown in the Supplemental Material [32].

*Collective spin dynamics.*—To examine the development of collective correlations in the dynamics, including the symmetrized off diagonal correlators, we study the Wineland spin squeezing parameter [44–46], defined as

$$\xi^2 \equiv \min_{\hat{n}} \frac{N \langle (\Delta \hat{S}_{\hat{n}})^2 \rangle}{|\langle \hat{S} \rangle|^2}. \quad (3)$$

Here,  $\langle (\Delta \hat{S}_{\hat{n}})^2 \rangle = \langle (\hat{S}_{\hat{n}} - \langle \hat{S}_{\hat{n}} \rangle)^2 \rangle$  is the transverse spin variance, with  $\hat{S}_{\hat{n}} = \hat{n} \cdot \hat{S}$ , minimized over all axes  $\hat{n}$  perpendicular to the collective Bloch vector  $\langle \hat{S} \rangle$ .  $\xi^2 < 1$  implies the presence of multipartite entanglement [47], and the scaling of the achievable spin squeezing with system size provides an indicator of collective behavior [12,24]. In addition, the spin squeezing quantifies the gain in angular resolution relative to its value for an uncorrelated coherent spin state. The sensitivity of the latter is bounded by the so-called standard quantum or shot-noise limit, given by  $\xi_{\text{SQL}}^2 = 1$ . A state with  $\xi^2 < 1$  is thus a potential resource for improved precision measurements [48].

In Fig. 1, we compare the performance of DTWA and GSE-TDVP in computing the spin squeezing dynamics for select values of  $\Delta$  and the power-law coupling  $\alpha$  for a  $6 \times 6$  and a  $10 \times 10$  system. Given the generic difficulty of simulating large system sizes, we only time evolve with GSE-TDVP until a local minimum in the spin squeezing is

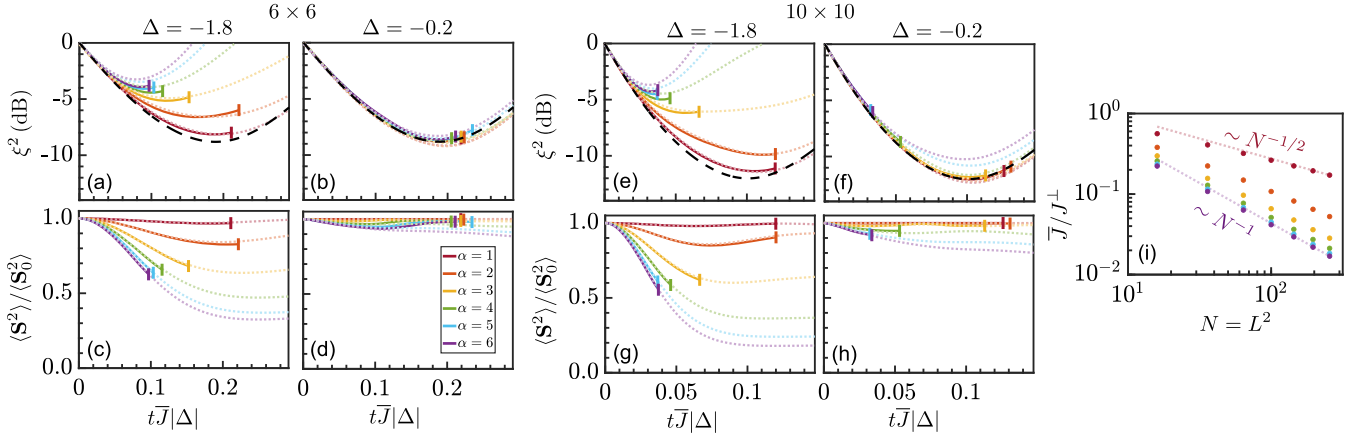


FIG. 1. Dynamics of (a),(b) the spin squeezing  $\xi^2$  (shown in decibels) and (c),(d) total spin  $\langle \hat{S}^2 \rangle$  generated by Eq. (1), shown for select interaction ranges  $\alpha$  and  $\Delta = -1.8, -0.2$  on a  $6 \times 6$  lattice. The total spin is normalized by its initial value,  $\langle \hat{S}^2 \rangle_0 = (N/2)(N/2 + 1)$ , and the time axis is scaled by the average spin interaction  $\bar{J}$  and  $|\Delta|$ . Solid lines are obtained by GSE-TDVP (longest evolved times denoted with vertical bars for visibility), while the dashed lines are obtained by DTWA. We show exact results for the collective case with  $\alpha = 0$  for comparison (black, dashed). (e)–(h) Analogous results for a  $10 \times 10$  lattice. (i) We also plot  $\bar{J}/J^\perp$  for various 2D square lattices of side length  $L$ , with expected power laws shown for comparison.

reached, when possible. We also rescale the time axis by  $|\Delta|\bar{J}$ , where  $\bar{J} = J^\perp \sum_{i \neq j} |\mathbf{r}_i - \mathbf{r}_j|^{-\alpha} / [N(N-1)]$  is the average interaction over all spin pairs. While this provides a convenient collapse of the dynamics at early times across our parameter space, we emphasize that “short” timescales under this rescaling generally do not correspond to short times in terms of the underlying Hamiltonian parameters, as can be observed from the magnitude of  $\bar{J}$  in Fig. 1(i).

Overall, we find that DTWA excellently captures the spin squeezing dynamics. While small numerical discrepancies  $\lesssim 0.5$  dB are observed in the minimum squeezing for larger  $\alpha$  when  $\Delta = -1.8$ , this offset appears to be constant for both system sizes in consideration. Furthermore, for smaller  $\alpha$  where we generally observe even better agreement, we find that any lingering discrepancies are somewhat smaller for the  $10 \times 10$  lattice, suggesting an improvement in accuracy as the size of the system is increased even beyond the reach of GSE-TDVP. In Figs. 1(c), 1(d), 1(g), and 1(h), we also compare the dynamics of the total collective spin length,  $\langle \hat{S}^2 \rangle$ , normalized by its initial value  $\langle \hat{S}_0^2 \rangle = (N/2)(N/2 + 1)$ , finding the dynamics are well captured by DTWA for all parameters and simulated times.

To make systematic comparisons over a wider swath of parameter space for Eq. (1), we utilize the optimal value of the spin squeezing (minimized over  $t$ ) as a figure of merit for the performance of DTWA relative to GSE-TDVP. In Figs. 2(a)–2(c), we plot the minimum squeezing over a range of  $\Delta$  and  $\alpha$  for lattice sizes up to  $10 \times 10$ . We continue to find that the general agreement of DTWA with GSE-TDVP persists across all parameters considered, including a slight improvement in agreement for small  $\alpha$  as the system size increases and a small, constant offset for larger  $\alpha$  and  $|\Delta|$ . For the region  $-2 \lesssim \Delta < 0$ , relatively

longer times are required to reach the minimum squeezing compared with other  $\Delta$ , and we also encounter a much larger bond dimension in this regime, particularly as  $\alpha$  is increased, as shown in the Supplemental Material [32]. Owing to the resource-intensive TDVP calculations for the large bond dimension, we only provide results when available.

Given the demonstrated correspondence between the spin squeezing dynamics for DTWA and GSE-TDVP, as well as the rare availability of exact results for a range of 2D system sizes beyond the capabilities of exact diagonalization, we examine the ability of DTWA to capture finite-size scaling trends. Of key importance for assessing the collective nature of the dynamics, as well as the achievable utility of these states for metrology, is the exponent  $\nu$  governing the system size dependence of the spin squeezing parameter [12,24,49],  $\xi^2 \sim N^\nu$ . In Fig. 2(d), we plot the values of this exponent as obtained from either DTWA or exact results for the displayed system sizes. We find good correspondence between these methods, which both capture the emergence of a quasicollective regime with enhanced  $|\nu|$  for  $\alpha < 4$  and small negative  $\Delta$ .

*Thermalization.*—To explore connections between the collective dynamics and the equilibrium physics of the XXZ model, we compare the long-time relaxation dynamics of Eq. (1) to the thermal ensemble at the same mean energy. Given the generic difficulty of both simulating long-time dynamics and accessing the low-temperature physics of the system, we employ a combination of phase space and MPS methods to explore this regime.

We can apply DTWA to efficiently compute the long-time dynamics of this system, though owing to the large growth of entanglement as the system approaches equilibrium, we are unable to make comparisons with equivalent



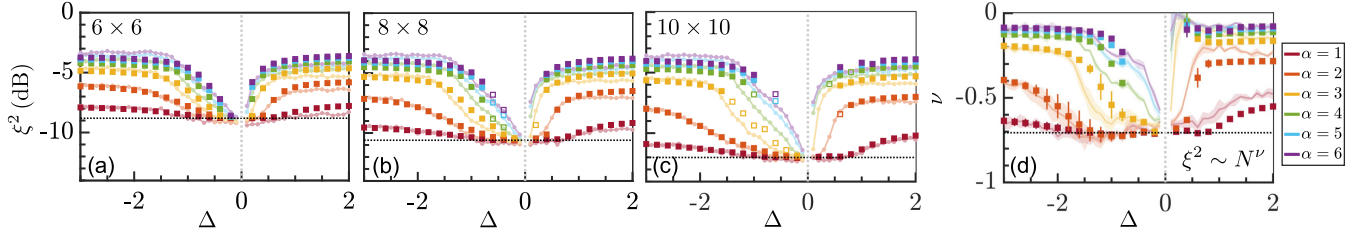


FIG. 2. (a)–(c) Optimal spin squeezing  $\xi^2$  (in decibels) computed via GSE-TDVP (squares) and DTWA (faded lines) for various 2D lattice sizes, interaction ranges  $\alpha$ , and  $\Delta$ . The dotted horizontal lines denote the expected results for the OAT model ( $\alpha = 0$ ), while the vertical dashed lines correspond to  $\Delta = 0$ . Unfilled squares denote estimated values for parameters where the GSE-TDVP dynamics approach close to, but do not achieve, a local minimum for the longest evolved times, as shown in the Supplemental Material [32]. (d) Fits for the power-law scaling of the optimal spin squeezing with the particle number  $N$ , where  $\xi^2 \sim N^\nu$ . The associated fitting error is denoted by error bars for exact results, or the shaded region for DTWA results. We supplement our data with exact and DTWA results for a  $4 \times 4$  lattice, and only provide fits when data for three or more system sizes are available.

MPS methods, even with the GSE variant of TDVP. We thus resort to comparisons with the corresponding thermal ensemble, computed via various MPS techniques: purification [50] and minimally entangled typical thermal states (METTS) [51,52]. Owing to the global conservation of  $\hat{S}_z$  by Eq. (1), we include an associated Lagrange multiplier in our thermal ensemble that properly accounts for local fluctuations of this quantity, and which should be adequate to describe the thermalized values of local observables. However, for the consideration of *global* correlators of the closed system, where  $\hat{S}_z$  is not allowed to fluctuate, we further modify our ensemble with an additional Lagrange multiplier to enforce conservation of the variance  $(\Delta \hat{S}_z)^2$ , as shown in the Supplemental Material [32].

In Fig. 3, we plot the value of the transverse magnetization  $\langle \hat{S}_\perp^2 \rangle$  for various scaled times as computed via DTWA, where  $\hat{\mathbf{S}}_\perp = (\hat{S}_x, \hat{S}_y, 0)$ , and compare this to the value in the associated thermal ensemble, obtained from MPS. We find that  $\langle \hat{S}_\perp^2 \rangle$  at the rescaled time  $t/t_{\text{OAT}}^* = 1$ , where  $t_{\text{OAT}}^*$  is the optimal squeezing time for an OAT model with coupling  $\chi = \bar{J}|\Delta|/2$ , appears to align closely with the thermal value when  $\Delta < 0$ . However, at later times, we observe that the value of  $\langle \hat{S}_\perp^2 \rangle$ , as computed via DTWA, continues to slowly decay for  $\alpha > 2$  and  $-2 \lesssim \Delta < 0$ , significantly deviating from the thermal expectation.

We attribute this artifact to a breakdown of DTWA at long times when thermalizing to the expected long-range or quasi-long-range ordered state—the *XY* ferromagnet characterized by a macroscopic transverse magnetization—for  $\alpha > 2$  and small negative  $\Delta$ , as opposed to any physical effect present in the actual system. Indeed, as  $\Delta$  approaches 0, the initial spin-polarized state tends to an eigenstate of the system, and should not undergo any spurious relaxation. Overall however, we find that DTWA at least plateaus to the expected thermal value initially, before exhibiting this further decay. For  $\Delta > 0$  and  $\Delta \lesssim -2$ , the relaxation at late times of DTWA agrees well with METTS and purification calculations.

In Fig. 3(c), we also plot the temperature of the thermal state obtained via purification or METTS, which we scale by  $\bar{J}$  to account for the possible superextensive scaling of

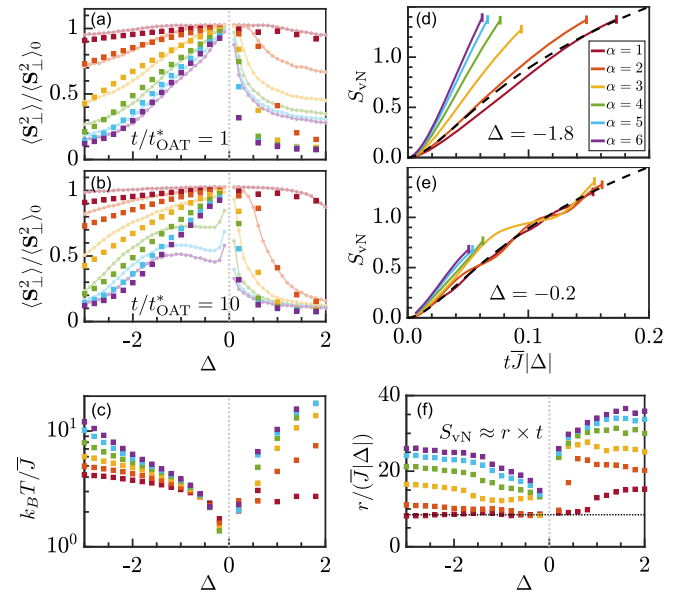


FIG. 3. (a),(b) Comparison between the long-time values (lines) and thermal ensemble averages (squares, same in each panel) of the transverse magnetization  $\langle \hat{S}_\perp^2 \rangle$ , normalized by its initial value of  $\langle \hat{S}_\perp^2 \rangle_0 = N(N+1)/4$  for a  $6 \times 6$  lattice. Dynamical results are obtained via DTWA for various scaled times  $t/t_{\text{OAT}}^*$ . The thermal averages are obtained via METTS for  $\Delta > 0$  and via a purification method for  $\Delta < 0$ . (c) We also show the temperature  $T$  of the thermal state, scaled by  $\bar{J}$ . (d),(e) Dynamical growth of the bipartite entanglement entropy,  $S_{vN} = -\text{Tr}[\hat{\rho}_A \ln \hat{\rho}_A]$ , where  $\hat{\rho}_A$  is the reduced density matrix for a bipartition of the lattice about the center. We show GSE-TDVP results on an  $8 \times 8$  lattice for various values of  $\Delta$  and  $\alpha$ , scaling the time axis by  $\bar{J}|\Delta|$ . We also provide the results for the OAT model (black, dashed) for comparison. (f) From the available short-time data, we estimate the growth rate of the entropy by fitting  $S_{vN} \approx r \times t$ , and plot the resulting coefficient  $r$ , scaled by  $\bar{J}|\Delta|$ . The resulting fit for the OAT model over the range  $t\bar{J}|\Delta| \lesssim 0.3$  is also shown (black, dotted).

Eq. (1). We can see that the onset of a large total spin in the late-time dynamics and corresponding thermal ensemble is linked closely with a reduction in temperature, as well as an enhanced scalability of the attainable spin squeezing in Fig. 2(d), suggesting the continuous-symmetry-broken low energy structure plays a critical role in the onset of collective squeezing behavior [12,21,24].

Finally, in Figs. 3(d)–3(f), we estimate the growth of the bipartite entanglement entropy over the 2D lattice from available GSE-TDVP dynamics, which is a quantity that remains inaccessible to DTWA. Close to  $\Delta = 0$ , we find that the entropy growth rate is similar for all  $\alpha$ , and collapses close to the expected entropy growth for the all-to-all case in our scaled time. This is consistent with the scrambling of the dynamics within the limited set of collective states. Away from  $\Delta = 0$ , we observe faster entanglement growth for shorter-ranged interactions, where the dynamics spreads beyond the collective manifold to the larger space of noncollective states. This regime coincides with an observed reduction in the scalability of the attainable spin squeezing, as well as with an increase in the size of the bond dimensions required to represent the state, as shown in the Supplemental Material [32]. Overall, we observe that an increased growth rate appears to be roughly associated with a higher final temperature of the corresponding thermal ensemble.

*Conclusions.*—We have demonstrated that DTWA provides efficient, accurate solutions for the dynamics of the 2D  $XXZ$  model with power-law decaying interactions through benchmarks with an extended TDVP algorithm, on lattice sizes of up to  $10 \times 10$ . These system sizes are directly relevant for current experiments utilizing trapped ions [25] or optical tweezer arrays of Rydberg atoms [26,27]. We have also probed the long-time relaxation of DTWA with MPS calculations of the expected thermal ensemble, finding good agreement at intermediate times and the ability to capture the onset of long-range or quasi-long-range order, while also demonstrating the continued utility of MPS methods for probing quantities inaccessible to DTWA, such as the entanglement growth.

We acknowledge helpful discussions with Chunlei Qu and Michael Perlin, as well as valuable feedback on the manuscript from David Wellnitz and Alexey Gorshkov. The MPS calculations were performed on the Vienna Scientific Cluster (VSC) using the ITensor [53] and ITensor/TDVP [19] library. A. M. R. and S. R. M. are supported by the AFOSR Grant No. FA9550-18-1-0319, the ARO single investigator Grant No. W911NF-19-1-0210, the NSF PHY1820885, NSF JILA-PFC PHY-2317149 and NSF QLCI-2016244 grants, by the DOE Quantum Systems Accelerator (QSA) grant, by the Vannevar Bush Faculty Fellowship (VBFF), and by NIST. M. Y. has received support from the European Research Council (ERC) under

the European Union’s Horizon 2020 research and innovation program through the ERC Consolidator Grant SEQUAM (Grant No. 863476). S. R. W. acknowledges the support of the NSF through Grant No. DMR-2110041.

\*These authors contributed equally to this work.

- [1] J. W. Britton, B. C. Sawyer, A. C. Keith, C. C. Wang, J. K. Freericks, H. Uys, M. J. Biercuk, and J. J. Bollinger, Engineered two-dimensional Ising interactions in a trapped-ion quantum simulator with hundreds of spins, *Nature (London)* **484**, 489 (2012).
- [2] P. Jurcevic, B. P. Lanyon, P. Hauke, C. Hempel, P. Zoller, R. Blatt, and C. F. Roos, Quasiparticle engineering and entanglement propagation in a quantum many-body system, *Nature (London)* **511**, 202 (2014).
- [3] C. D. Bruzewicz, J. Chiaverini, R. McConnell, and J. M. Sage, Trapped-ion quantum computing: Progress and challenges, *Appl. Phys. Rev.* **6**, 021314 (2019).
- [4] J. L. Bohn, A. M. Rey, and J. Ye, Cold molecules: Progress in quantum engineering of chemistry and quantum matter, *Science* **357**, 1002 (2017).
- [5] S. A. Moses, J. P. Covey, M. T. Miecnikowski, D. S. Jin, and J. Ye, New frontiers for quantum gases of polar molecules, *Nat. Phys.* **13**, 13 (2017).
- [6] L. Chomaz, I. Ferrier-Barbut, F. Ferlaino, B. Laburthe-Tolra, B. L. Lev, and T. Pfau, Dipolar physics: A review of experiments with magnetic quantum gases, *Rep. Prog. Phys.* **86**, 026401 (2023).
- [7] A. Browaeys and T. Lahaye, Many-body physics with individually controlled Rydberg atoms, *Nat. Phys.* **16**, 132 (2020).
- [8] S. Lepoutre, J. Schachenmayer, L. Gabardos, B. Zhu, B. Naylor, E. Marechal, O. Gorceix, A. M. Rey, L. Vernac, and B. Laburthe-Tolra, Out-of-equilibrium quantum magnetism and thermalization in a spin-3 many-body dipolar lattice system, *Nat. Commun.* **10**, 1714 (2019).
- [9] U. Schollwöck, The density-matrix renormalization group in the age of matrix product states, *Ann. Phys. (Amsterdam)* **326**, 96 (2011), January 2011 Special Issue.
- [10] B. Tang, E. Khatami, and M. Rigol, A short introduction to numerical linked-cluster expansions, *Comput. Phys. Commun.* **184**, 557 (2013).
- [11] K. R. A. Hazzard *et al.*, Many-Body Dynamics of Dipolar Molecules in an Optical Lattice, *Phys. Rev. Lett.* **113**, 195302 (2014).
- [12] T. Comparin, F. Mezzacapo, and T. Roscilde, Robust spin squeezing from the tower of states of  $U(1)$ -symmetric spin Hamiltonians, *Phys. Rev. A* **105**, 022625 (2022).
- [13] R. Menu and T. Roscilde, Gaussian-state Ansatz for the non-equilibrium dynamics of quantum spin lattices, *SciPost Phys.* **14**, 151 (2023).
- [14] A. Polkovnikov, Phase space representation of quantum dynamics, *Ann. Phys. (Amsterdam)* **325**, 1790 (2010).
- [15] J. Schachenmayer, A. Pikovski, and A. M. Rey, Many-Body Quantum Spin Dynamics with Monte Carlo Trajectories on a Discrete Phase Space, *Phys. Rev. X* **5**, 011022 (2015).
- [16] L. Pucci, A. Roy, and M. Kastner, Simulation of quantum spin dynamics by phase space sampling of

- Bogoliubov-Born-Green-Kirkwood-Yvon trajectories, *Phys. Rev. B* **93**, 174302 (2016).
- [17] J. Wurtz, A. Polkovnikov, and D. Sels, Cluster truncated Wigner approximation in strongly interacting systems, *Ann. Phys. (Amsterdam)* **395**, 341 (2018).
- [18] B. H. Zhu, A. M. Rey, and J. Schachenmayer, A generalized phase space approach for solving quantum spin dynamics, *New J. Phys.* **21**, 45 (2019).
- [19] M. Yang and S. R. White, Time-dependent variational principle with ancillary Krylov subspace, *Phys. Rev. B* **102**, 094315 (2020).
- [20] M. P. Kwasirogroch and N. R. Cooper, Synchronization transition in dipole-coupled two-level systems with positional disorder, *Phys. Rev. A* **96**, 053610 (2017).
- [21] M. A. Perlin, C. Qu, and A. M. Rey, Spin Squeezing with Short-Range Spin-Exchange Interactions, *Phys. Rev. Lett.* **125**, 223401 (2020).
- [22] T. Bilitewski, L. De Marco, J.-R. Li, K. Matsuda, W. G. Tobias, G. Valtolina, J. Ye, and A. M. Rey, Dynamical Generation of Spin Squeezing in Ultracold Dipolar Molecules, *Phys. Rev. Lett.* **126**, 113401 (2021).
- [23] J. T. Young, S. R. Muleady, M. A. Perlin, A. M. Kaufman, and A. M. Rey, Enhancing spin squeezing using soft-core interactions, *Phys. Rev. Res.* **5**, L012033 (2023).
- [24] M. Block, B. Ye, B. Roberts, S. Chern, W. Wu, Z. Wang, L. Pollet, E. J. Davis, B. I. Halperin, and N. Y. Yao, A universal theory of spin squeezing, [arXiv:2301.09636](https://arxiv.org/abs/2301.09636).
- [25] J. Franke, S. R. Muleady, R. Kaubruegger, F. Kranzl, R. Blatt, A. M. Rey, M. K. Joshi, and C. F. Roos, Quantum-enhanced sensing on optical transitions through finite-range interactions, *Nature (London)* **621**, 740 (2023).
- [26] G. Bornet, G. Emperauger, C. Chen, B. Ye, M. Block, M. Bintz, J. A. Boyd, D. Barredo, T. Comparin, F. Mezzacapo, T. Roscilde, T. Lahaye, N. Y. Yao, and A. Browaeys, Scalable spin squeezing in a dipolar Rydberg atom array, *Nature* **621**, 728 (2023).
- [27] W. J. Eckner, N. D. Oppong, A. Cao, A. W. Young, W. R. Milner, J. M. Robinson, J. Ye, and A. M. Kaufman, Realizing spin squeezing with Rydberg interactions in a programmable optical clock, *Nature* **621**, 734 (2023).
- [28] H. Ozawa, S. Taie, Y. Takasu, and Y. Takahashi, Hybrid quantum system of fermionic neutral atoms in a tunable optical lattice, in *Hybrid Quantum Systems*, Quantum Science and Technology, edited by Y. Hirayama, K. Ishibashi, and K. Nemoto (Springer Nature, Singapore, 2021), pp. 219–243, [10.1007/978-981-16-6679-7\\_10](https://doi.org/10.1007/978-981-16-6679-7_10).
- [29] M. Kitagawa and M. Ueda, Squeezed spin states, *Phys. Rev. A* **47**, 5138 (1993).
- [30] M. Foss-Feig, K. R. A. Hazzard, J. J. Bollinger, A. M. Rey, and C. W. Clark, Dynamical quantum correlations of Ising models on an arbitrary lattice and their resilience to decoherence, *New J. Phys.* **15**, 113008 (2013).
- [31] J. Schachenmayer, A. Pikovski, and A. M. Rey, Dynamics of correlations in two-dimensional quantum spin models with long-range interactions: A phase-space Monte-Carlo study, *New J. Phys.* **17**, 065009 (2015).
- [32] See Supplemental Material at <http://link.aps.org/supplemental/10.1103/PhysRevLett.131.150401> for additional details regarding the implementation of DTWA, GSE-TDVP, purification, and METTS, and which includes Refs. [33–37].
- [33] M. P. Zaletel, R. S. K. Mong, C. Karrasch, J. E. Moore, and F. Pollmann, Time-evolving a matrix product state with long-ranged interactions, *Phys. Rev. B* **91**, 165112 (2015).
- [34] W. Morong, S. R. Muleady, I. Kimchi, W. Xu, R. M. Nandkishore, A. M. Rey, and B. DeMarco, Disorder-controlled relaxation in a three-dimensional Hubbard model quantum simulator, *Phys. Rev. Res.* **3**, L012009 (2021).
- [35] Y. A. Alaoui, B. Zhu, S. R. Muleady, W. Dubosclard, T. Roscilde, A. M. Rey, B. Laburthe-Tolra, and L. Vernac, Measuring Correlations from the Collective Spin Fluctuations of a Large Ensemble of Lattice-Trapped Dipolar Spin-3 Atoms, *Phys. Rev. Lett.* **129**, 023401 (2022).
- [36] F. Verstraete, J. J. García-Ripoll, and J. I. Cirac, Matrix Product Density Operators: Simulation of Finite-Temperature and Dissipative Systems, *Phys. Rev. Lett.* **93**, 207204 (2004).
- [37] S. R. White, Density Matrix Formulation for Quantum Renormalization Groups, *Phys. Rev. Lett.* **69**, 2863 (1992).
- [38] M. Babadi, E. Demler, and M. Knap, Far-from-Equilibrium Field Theory of Many-Body Quantum Spin Systems: Prethermalization and Relaxation of Spin Spiral States in Three Dimensions, *Phys. Rev. X* **5**, 041005 (2015).
- [39] A. Schuckert, I. Lovas, and M. Knap, Nonlocal emergent hydrodynamics in a long-range quantum spin system, *Phys. Rev. B* **101**, 020416(R) (2020).
- [40] M. Kunimi, K. Nagao, S. Goto, and I. Danshita, Performance evaluation of the discrete truncated Wigner approximation for quench dynamics of quantum spin systems with long-range interactions, *Phys. Rev. Res.* **3**, 013060 (2021).
- [41] P. Kramer and M. Saraceno, The time-dependent variational principle (TDVP), in *Geometry of the Time-Dependent Variational Principle in Quantum Mechanics*, Lecture Notes in Physics, (Springer, Berlin, Heidelberg, 1981), pp. 3–14, [10.1007/3-540-10579-4\\_20](https://doi.org/10.1007/3-540-10579-4_20).
- [42] J. Haegeman, J. I. Cirac, T. J. Osborne, I. Pižorn, H. Verschelde, and F. Verstraete, Time-Dependent Variational Principle for Quantum Lattices, *Phys. Rev. Lett.* **107**, 070601 (2011).
- [43] J. Haegeman, C. Lubich, I. Oseledets, B. Vandereycken, and F. Verstraete, Unifying time evolution and optimization with matrix product states, *Phys. Rev. B* **94**, 165116 (2016).
- [44] D. J. Wineland, J. J. Bollinger, W. M. Itano, F. L. Moore, and D. J. Heinzen, Spin squeezing and reduced quantum noise in spectroscopy, *Phys. Rev. A* **46**, R6797 (1992).
- [45] D. J. Wineland, J. J. Bollinger, W. M. Itano, and D. J. Heinzen, Squeezed atomic states and projection noise in spectroscopy, *Phys. Rev. A* **50**, 67 (1994).
- [46] J. Ma, X. Wang, C. P. Sun, and F. Nori, Quantum spin squeezing, *Phys. Rep.* **509**, 89 (2011).
- [47] A. S. Sorensen and K. Molmer, Entanglement and Extreme Spin Squeezing, *Phys. Rev. Lett.* **86**, 4431 (2001).
- [48] L. Pezzé, A. Smerzi, M. K. Oberthaler, R. Schmied, and P. Treutlein, Quantum metrology with nonclassical states of atomic ensembles, *Rev. Mod. Phys.* **90**, 035005 (2018).
- [49] M. Foss-Feig, Z.-X. Gong, A. V. Gorshkov, and C. W. Clark, Entanglement and spin-squeezing without infinite-range interactions, [arXiv:1612.07805](https://arxiv.org/abs/1612.07805).

- [50] A. E. Feiguin and S. R. White, Time-step targeting methods for real-time dynamics using the density matrix renormalization group, *Phys. Rev. B* **72**, 020404(R) (2005).
- [51] S. R. White, Minimally Entangled Typical Quantum States at Finite Temperature, *Phys. Rev. Lett.* **102**, 190601 (2009).
- [52] E. M. Stoudenmire and S. R. White, Minimally entangled typical thermal state algorithms, *New J. Phys.* **12**, 055026 (2010).
- [53] M. Fishman, S. R. White, and E. M. Stoudenmire, The ITensor software library for tensor network calculations, *SciPost Phys. Codebases* 4 (2022).